Three-dimensional crack monitoring through a transparent replica of brittle rock manufactured with fused quartz

H Li[1], G Q Kong[2*], H Y Qin[3], H Abuel-Naga[4], J L Li[5], and Q Yang[6]

[1] College of Civil Engineering and Architecture, Wenzhou University, Wenzhou, China
[2] College of Civil and Transportation Engineering, Hohai University, Nanjing, China
[3] School of Computer Science, Engineering and Mathematics, Flinders University, SA, Australia
[4] School of Engineering and Mathematical Sciences, La Trobe University, Melbourne, Australia
[5] Department of Mechanical and Civil Engineering, Purdue University Northwest, Westville and Hammond, Indiana, America
[6] School of Civil Engineering, Dalian University of Technology, Dalian, China

[*] Correspondence to: Xikang Road No. 1, Nanjing 210098, China. E-mail address: gqkong@hhu.edu.cn, Tel: (86) 15205168312, ORCID: 0000-0002-0645-5140, (G. Q. Kong).

Abstract. Transparent rock-like materials have been used as a replica of natural rock to study the crack propagation mechanisms. Previous research focused on materials such as glass or transparent polymethyl methacrylate. In this paper, an alternative transparent material that is manufactured with fused quartz was presented, along with the manufacturing process and deformation behavior during a uniaxial compression test. Three digital cameras were arranged around the specimen during the uniaxial compression test to capture the cracks of the same moment from different angles for 3D reconstruction of the cracks. Results show that fused quartz has a similar deformation behavior as natural brittle rock and has potential for the reconstruction of 3D cracks in rocks for quantitative analysis of crack propagation.

1. Introduction

Brittle failure of rocks is one of the most important issues in fracture mechanics. Most previous research on rock cracks focused on the expansion of two-dimensional (2D) cracks [1-3]. However, this issue belongs to the space problem in practical projects. Studying the expansion of three-dimensional (3D) cracks in rocks is difficult due to their opacity. Related methods include computed tomography (CT), acoustic emission (AE), nuclear magnetic resonance imaging (NMRI), and infrared spectroscopy, with the latter being used more frequently to study 3D crack expansion [4-5]. However, the accuracy of AE and infrared spectroscopy is relatively low, and their result can be used only as a supplement of the monitored phenomenon. Although CT and NMRI can achieve real-time and relatively high-accuracy results, their complexity and high cost limit their use.

One effective method is to use transparent rock-like materials to observe the formation and evolution of 3D cracks; this approach is usually simple, quick, and inexpensive. Glass [6], resins [7], and polymethyl methacrylate [8-9] are typical transparent materials used to represent brittle rocks.

However, these materials all have disadvantages in terms of brittleness or transparency, thereby limiting their application in visual tests. Fused quartz particle mixture with refractive index-matched pore fluid, which has high transparency and mechanical properties that are more similar to those of natural sand, is one of the suitable transparent replicas of sand [10]. Whether fused quartz blocks can be used as transparent replica of brittle rocks is worth studying, and its application prospects are also worth discussing.

Hence, the preparation method of fused quartz block sample, which was used as a potential substitute for natural rock, was introduced in this paper. Experiments on the deformation behavior of transparent silica blocks were performed under uniaxial compressive loading. A preliminary attempt at 3D crack reconstruction was conducted based on stereo vision principle to demonstrate the potential application of the transparent silica block on the study of 3D crack expansion pattern.

2. Materials and methods

The transparent specimens used in this investigation are purified fused quartz, which comprises approximately 99.700% silicon dioxides, 0.002% ferric oxide, and 0.298% other ingredients. This material has a similar physical property as rocks, stable chemical properties, and high brittleness that makes it suitable for replacing natural brittle rocks. Figure 1 shows the specimen preparation process, and the steps are listed as follows:

(1) Natural crystalline silica materials were first crushed and soaked with hydrochloric acid for 24–48 h to preliminarily remove acid-soluble impurities.

(2) After preliminary purification, the silica particles were melted at 1600℃–2000℃ for 6–8 h. During the melting process, activated carbon rod and alumina materials were placed around the material to absorb absorbable impurities.

(3) After being melted, the silica materials were cooled down and crushed into particles. Then, the crushed particles were soaked with hydrochloric acid. Steps (2) and (3) were repeated until the major impurities were removed.

(4) The liquid quartz obtained from the last molten process was cooled down in a mold with the corresponding size of the test design. The specimen was obtained after cutting, grinding, and polishing.

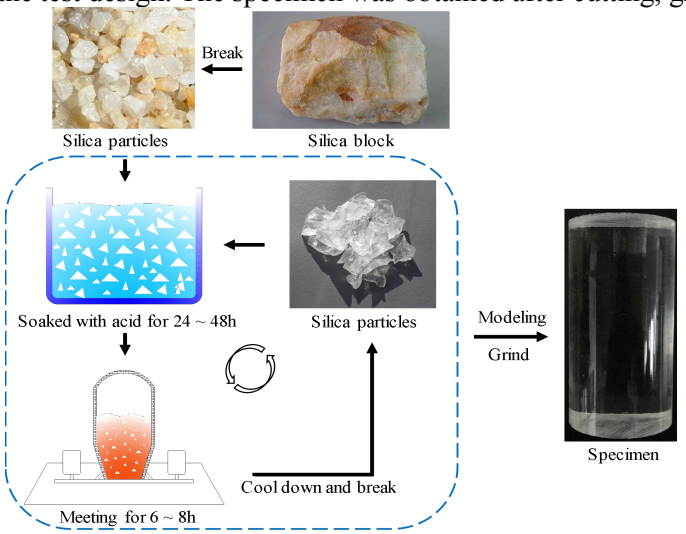

Figure 1. Illustration of specimen preparation.

Four specimens were prepared according to the suggested methods for determining uniaxial compressive strength (UCS) to experimentally examine the strength and deformation behavior of the transparent rock-like material [11]. The specimens were made into right circular cylinders that have a diameter of 50 mm and a height-to-diameter ratio of 2. The dimensions, density, and P-wave velocity of each specimen are listed in Table 1.

Uniaxial compressive loading was conducted by using an RMT-150C multifunction automatically rigid servo testing machine. A schematic of the test facilities is shown in Figure 2. The specimen was sandwiched between two loading plates with matching sizes. Vaseline was evenly applied to the contact surfaces between the ends of specimen and the loading platens to reduce the end effect. The loading is applied by a hydraulic servo-system in a displacement control manner at 0.01 mm/s. The loading, axial, and lateral displacement were measured and stored during loading. Three digital cameras were used to capture cracks in specimens from different directions during loading. The location of the cameras is shown in Figure 2. The photos from the cameras were used for the reconstruction of 3D cracks. The distance from the lens to the specimen center was controlled at 600 mm for all the cameras; this distance was selected to ensure accuracy and reduce perspective distortions of the photos. The angle between cameras was selected according to the actual situation of the laboratory to ensure that the cameras were not shielded during shooting and the calculation of the later image matching was convenient.

Table 1. Dimensions, basic physical, and experimental results of the specimens.

No.	Diameter (mm)	Height (mm)	Density (g/cm^3)	P-wave velocity	E_P (GPa)	v	UCS (MPa)
S1	50.13	98.95	2.211	6008.49	66.86	0.066	135.74
S2	50.00	98.97	2.215	5892.06	61.17	0.090	161.63
S3	49.71	99.37	2.209	6022.22	64.62	0.027	92.67
S4	49.94	99.00	2.203	6073.62	/	/	/

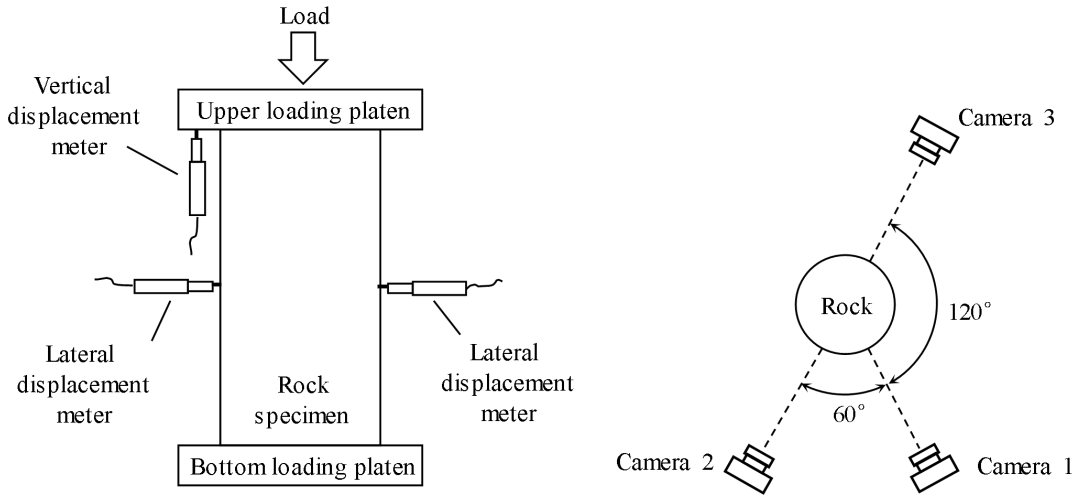

Figure 2. Schematic of experimental setup.

3. Results and analysis

3.1. Uniaxial compressive test

The stress–strain curves of the specimens, except S4, are presented in Figure 3. S4 is used for 3D reconstruction of cracks after loading. However, a large number of cracks appeared in the sample when the load increased to a certain extent, thereby causing great difficulty to 3D reconstruction of the cracks. Thus, S4 was not loaded to damage and the stress–strain curve is not displayed in Figure 3. Generally, these curves follow a consistent manner before the peak stress and may be divided into four parts (compaction, elastic region, stable crack growth, and post-peak deformation) according to the crack initiation process observed during the test. Initially, a nonlinear segment exists, which represents the gradual connection of the specimen and the instrument. Elastic deformation takes place after the nonlinear deformation, and the elastic modulus and Poisson's ratio can be determined from this region.

The elastic modulus of S1, S2, and S3 is 66.86, 61.17, and 64.62 GPa, respectively, which is within the range of the plagioclase granite of 61.09–73.98 GPa [12]. However, the Poisson's ratios of the specimens are 3 to 4 times lower than that of plagioclase granite (Table 1).

The axial stress level where the total volumetric strain reversal occurs represents the beginning of unstable crack growth. However, the reversal of the total volumetric strain is not observed for this material, which may be caused by the low Poisson's ratios. Thus, this paper established that crack damage stress (σ_{cd}) is equal to peak strength (σ_f) because four regions exist and not five [5]. This phenomenon was also recorded by Martin and Chandler [2] over a series of tests with a slow loading rate. Beyond the peak stress, the axial stress versus axial strain shows a rapid decrease, as shown in Figure 3. The stress–strain relationships of charcoal gray granite, Westerly granite, and Beishan granite [13-15] are also plotted in Figure 3 for comparison. The figure shows that the stress–strain relationships of the specimens are similar to those of the brittle rocks.

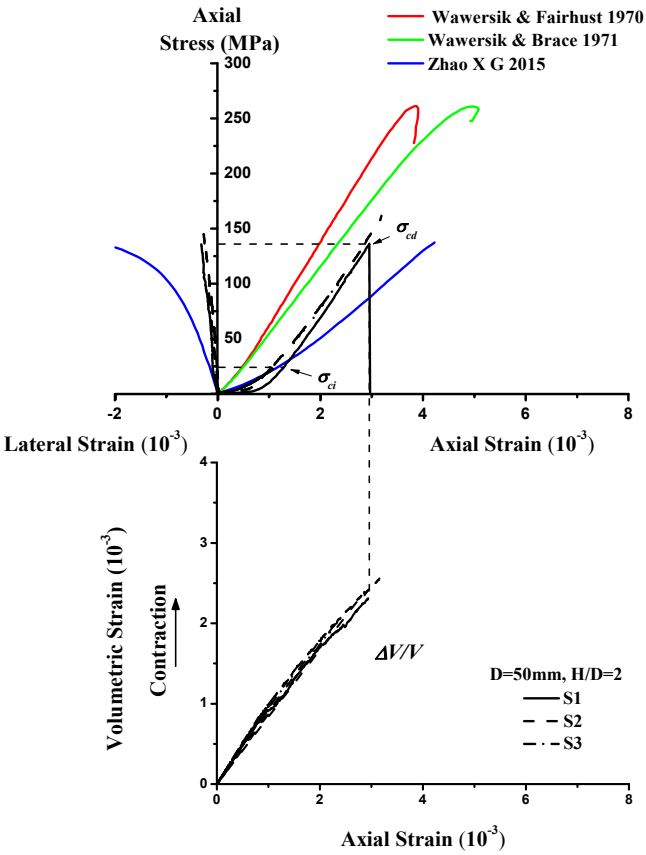

Figure 3. Curves on stress versus strain of the specimens.

The measured values of the UCS of specimen S1, S2, and S3 are 135.74, 161.63, and 92.67 MPa as shown in Table 1, which are within the range of 100–250 MPa of granite. However, a large diversity exists among the UCS of S1, S2, and S3. This result may be caused by the anisotropy and minor impairment of the specimens during the manufacturing and grinding processes.

3.2. 3D reconstruction of cracks

The 3D reconstruction of the cracks inside the transparent silica specimen was preliminarily performed based on the structure from motion (SFM) technique [16]. The pairs of 2D image coordinate (*u, v*), from the corresponding camera sensors, were reproduced to a single set of 3D global coordinates (*x, y, z*) using the function (1)

$$Z_c \begin{bmatrix} u \\ v \\ 1 \end{bmatrix} = KA \begin{bmatrix} x \\ y \\ z \\ 1 \end{bmatrix} \quad \text{* MERGEFORMAT (1)}$$

where Zc is the distance between the observation point and the camera; K is the camera intrinsic parameter matrix; and A is the camera extrinsic parameter matrix. The parameters of K and A can be determined according to Debevec [17].

Each camera's set of 2D image coordinates was transformed separately, and three sets of 2D global coordinates were obtained. Corresponding two sets of points in the three sets were interpolated to produce a set of final 3D coordinates. Figure 4a shows the crack distribution in S4 through 3D reconstruction. Crack planes ①, ②, and ③ were formed by wing cracks of S4 (Figure 4b). The orientation of crack planes tends to the loading direction as the loading increases. 3D reconstruction was also conducted for other key stages of loading, as shown in Figure 4b. The 3D reconstruction images were compared with the physical photos of the specimen. The reconstruction image agrees well with the real situation. In this part, the load was stopped at an early age because the cracks cover each other, thus making the 3D reconstruction of the cracks difficult.

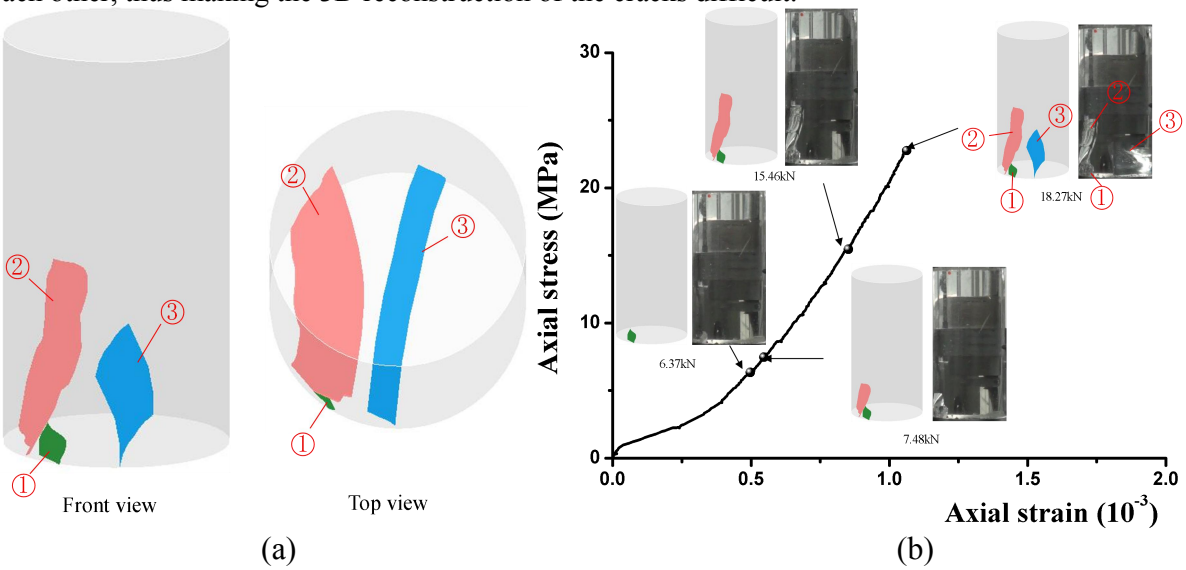

Figure 4. Propagation form of 3D crack of S4: (a) 3D reconstruction of cracks; (b) propagation form of 3D cracks following loading.

4. Discussion

The transparent rock-like material has broad application prospects. For the unit test, prefabricated cracks can be embedded in the transparent rock-like material to study the propagation principle of the 3D cracks under complex stress. In combination with 3D printing technology, different types of transparent rock-like masses can be prefabricated, and the interaction between transparent rock-like masses and structures can be studied.

5. Conclusions

A transparent rock-like material that is a potential substitute for natural brittle rock is described in this paper, and its manufacturing method and deformation behavior during the uniaxial compression test are included. A brief 3D crack reconstruction in the transparent specimen is preliminarily attempted. The following conclusions were obtained: The stress–strain curves of fused quartz blocks have a similar trend to that of the natural brittle rocks. The average modulus of the specimens is 64.21 GPa, which is within the range of granite of 61.09–73.98 GPa. However, the Poisson's ratio of this

material is 3 to 4 times smaller than that of granite. The average UCS of the transparent silica blocks is about 130 MPa, which is within the range of the normal granite strength of 100–250 MPa. The 3D cracks can be successfully and consistently established based on stereoscopic vision. The fused quartz shows potential for the 3D reconstruction of crack in transparent specimens. However, this material is mainly composed of silica, which is different from natural rocks, which are composed of a variety of minerals. The 3D reproduction of internal cracks on the basis of SFM is limited to the early stages of fracture due to the difficulty of matching the same point of crack in different photos when a large number of cracks are present.

References

[1] Hoek E and Bieniawski Z T 1965 Brittle fracture propagation in rock under compression. *Int. J. Fracture* **1(3)** 137–155.
[2] Martin C D and Chandler N A 1994 The progressive fracture of Lac du Bonnet granite. *Int. J. Rock Mech. Min.* **31(6)** 643–659.
[3] Haeri H, Shahriar K, Marji M F and Moarefvand P 2014 Experimental and numerical study of crack propagation and coalescence in pre-cracked rock-like disks. *Int. J. Rock Mech. Min.* **67** 20–28.
[4] Keller A 1998 High resolution, non-destructive measurement and characterization of fracture apertures. *Int. J. Rock Mech. Min.* **35(8)** 1037–1050.
[5] Yang S Q, Jing H W and Wang S Y 2012 Experimental investigation on the strength, deformability, failure behavior and acoustic emission locations of red sandstone under triaxial compression. *Rock Mech. Rock Eng.* **45(4)** 583–606.
[6] Wachtman J B 1974 Highlights of progress in the science of fracture of ceramics and glass. *J. Am. Ceram. Soc.* **57(12)** 509–519.
[7] Dyskin A V, Jewell R J, Joer H, Sahouryeh E and Ustinov K B 1994 Experiments on 3D crack growth in uniaxial compression. *Int. J. Fracture* **65(4)** 77-83.
[8] Germanovich L N, Salganik R L, Dyskin A V and Lee K K 1994 Mechanisms of brittle fracture of rock with pre-existing cracks in compression. *Pure Appl. Geophys.* **143(1-3)** 117-149.
[9] Wong R H C, Law C M, Chau K T and Zhu W S 2004 Crack propagation from 3-D surface fractures in PMMA and marble specimens under uniaxial compression. *Int. J. Rock Mech. Min.* **41(Suppl. 1)** 37–42.
[10] Kong G Q, Zhou L D, Wang Z T, Yang G and Li H 2016 Shear modulus and damping ratios of transparent soil manufactured by fused quartz. *Mater. Lett.* **182(1)** 257–259.
[11] ISRM 1979 Suggested method for determining deformability of rock materials in uniaxial compression. 138–140.
[12] Jaeger J C, Cook N G and Zimmerman R W 2007 *Fundamentals of rock mechanics*. Hoboken: Blackwell Publishing.
[13] Wawersik W R and Fairhurst C 1970 A study of brittle rock fracture in laboratory compression experiments. *Int. J. Rock Mech. Min.* **7(5)** 561–575.
[14] Wawersik W R and Brace W F 1971 Post-failure behavior of a granite and diabase. *Rock Mech. Rock Eng.* **3(2)** 61–85.
[15] Zhao X G, Cai M, Wang J and Li P F 2015 Strength comparison between cylindrical and prism specimens of Beishan granite under uniaxial compression. *Int. J. Rock Mech. Min.* **76** 10–17.
[16] Schönberger J L and Frahm J M 2016 Structure from motion revisited. *Proceedings of the IEEE Conference on Computer Vision and Pattern Recognition*, 4104-4113.
[17] Debevec P E 1996 *Modeling and rendering architecture from photographs* University of California Berkeley.